THE MONTEFERRATO SERPENTINIZED PERIDOTITE (FIGLINE DI PRATO, PRATO) IN THE NORTHERN APENNINES, ITALY: A WITNESS OF THE LIGURIAN OCEAN MARGIN IN THE MONUMENTAL RELIGIOUS BUILDINGS OF TUSCANY

Massimo Coli*,✉, Roberto Compagnoni**, Roberto Cossio**,***, Chiara Del Ventisette* and Paola Vannucchi*

* *Dept. Earth Sciences, Florence University, Firenze, Italy.*
** *Dept. Earth Sciences, Turin University, Torino, Italy.*
*** *"G. Scansetti" Interdepartmental Center for Studies on Asbestos and Other Toxic Particulates, University of Turin, Italy.*
✉ *Corresponding author, email: massimo.coli@unifi.it*

ABSTRACT

The Monteferrato area is the source site of "Verde Prato" that, together with Carrara Marble, forms the visual duotone that typifies Renaissance buildings in Tuscany. Verde Prato is a serpentinized peridotite that crops out close to Figline di Prato. At the beginning of the 20th century, Gustav Steinmann visited and described the ophiolitic outcrops of Figline di Prato, which contributed to his recognition of the "Steinmann Trinity", i.e., the common co-occurrence of serpentinites, pillow basalts and cherts. The Steinmann Trinity concept, in turn, formed an essential step in the development of ophiolite theories, sea-floor spreading, and plate tectonics. Because of the cultural, artistic and geologic importance of the Monteferrato serpentinized peridotite, the Tuscan Region classified these quarries as historical sites in its list of the Historical Ornamental Stones Quarries.

Within the Monteferrato serpentinites, large portions of the original peridotite are locally partially preserved, still presenting original microstructure of the mantle protolith. These peridotites preserve vestiges of sub-continental mantle deformation that occurred during the early stages of lithosphere extension, which opened the Ligurian Tethys in the Early Jurassic. Static crystallization of peridotitic minerals was followed by bulk serpentinization. Successive veins formed, filled by chrysotile and lizardite, with the former cutting the latter. Antigorite is also present in veins, but crosscutting relationships with the other veins are unclear. A tentative interpretation of the veining events relates the antigorite vein formation associated with the gabbro intrusions into the serpentinized peridotite, while the transition from chrysotile to lizardite relates to the activation of an extensional tectonic regime, perhaps linked to the closure of the Ligurian Tethys and bending of the subducting plate. Serpentinization may also provide the key to understand how the Monteferrato peridotites were ultimately emplaced within the Monte Morello Unit.

INTRODUCTION

"Verde Prato" is the vernacular name for the landmark ornamental building stone that has been used in Tuscany since the 11th century to form the dark-green that contrasts with white Carrara Marble in the spectacular duotone decorations that highlight and typify many historical Tuscan buildings (Fig. 1, Table 1) (Rodolico, 1965; Sartori, 2002; Malesani et al., 2003; Bastogi and Fratini, 2004; Fratini and Rescic, 2013).

Recent conservation-related interventions have led to a new interest in the geological characteristics of the type locality of this stone, which was quarried from an ophiolite body in Monteferrato near Prato (WGS84 43°55'41.33"N 11°4'22.08"E; Figs. 2 and 3). Its source ophiolite also played a key role in the development of the modern ophiolite hypothesis, being the Apennine area used to describe the "Steinmann Trinity" (Steinmann, 1913).

Historically, "Verde Prato" was mainly exploited in the Pian di Gello and Corsini quarries (Fig. 3) on the north-eastern slope of Monteferrato, where the least deformed serpentinized peridotites are exposed. In its plan for the quarrying activities, the Tuscany Region has included these quarries in the category of Historical Quarries (http://www502.regione.toscana.it/geoscopio/pianocave.html). Serpentinized peridotites were also quarried in other localities in Tuscany, such as Impruneta (south of Florence), Vallerano (near Siena), and near Volterra, but these quarries did not have the same

commercial value. In the second half of the 20th century, the northwestern side of the Monteferrato ophiolite body was quarried (Volpaie, Guarino and Montemezzano quarries, Fig. 3) to obtain material to be used as rock fill. All quarries fell into disuse in the 1990s since they contain widespread chrysotile asbestos.

In this paper, in part motivated by the necessity to use "Verde Prato" for building conservation purposes, we present further study on the petrologic characteristics of this stone. Our new results have also led us to propose a new hypothesis for their geological evolution and emplacement.

GEOLOGICAL SETTING

The ophiolites of Monteferrato form part of the Monte Morello Unit, the lowermost tectonic slice of the Ligurian Units. They were derived from the floor of the Alpine Tethys also known as the Liguria-Piemonte Ocean (Treves, 1984; Marroni and Pandolfi, 2007). Ligurian Units were then overthrust on top of the Tuscan Nappe, which derived from the continental margin during the Apennine orogenic phase (Boccaletti and Coli, 1983; Abbate et al., 1994).

The Liguria-Piemonte Ocean formed during the Late Jurassic (Elter, 1975; Abbate et al., 1980) because of the opening of the Central Atlantic Ocean, which separated Europe from Africa (Schettino and Turco, 2011). Tectonic and pet-

Fig. 1 - Examples of the Tuscan duotone cladding in white and dark marble: a) San Miniato al Monte, Florence; b) Cathedral, Prato; c) the religious complex constituted by the Saint John Baptistery, the Santa Maria del Fiore Cathedral and the Giotto's Bell-Tower, Florence; d) the façade of the Santa Croce Basilica, Florence; e) Verde Prato quoins in the façade of the lateral Cathedral of Prato; f) detail of Verde Prato in the cladding of the Saint John Baptistery, Florence (pictures by Massimo Coli).

rologic characteristics of the oldest ophiolites of the Northern Apennines indicate that rifting occurred along non-volcanic margins, and was associated with the exposure of sub-continental serpentinized peridotites (Molli, 1996; Marroni et al., 1998; 2002; Tribuzio et al., 2004). The Liguria-Piemonte Ocean was characterized by slow spreading rates (Lagabrielle and Cannat, 1990) and diffuse transform faults/fracture zones oriented at a low angle with respect to the continental boundaries (Abbate et al., 1980; Boccaletti et al., 1984; Abbate and Bortolotti, 1984; Nirta et al., 2007). This setting caused exposure to the ocean floor of serpentinized mantle peridotites, with uplifted oceanic basement rocks inferred along fracture zones of the Liguria-Piemonte Ocean, while the rough topography of the ocean floor led to the formation
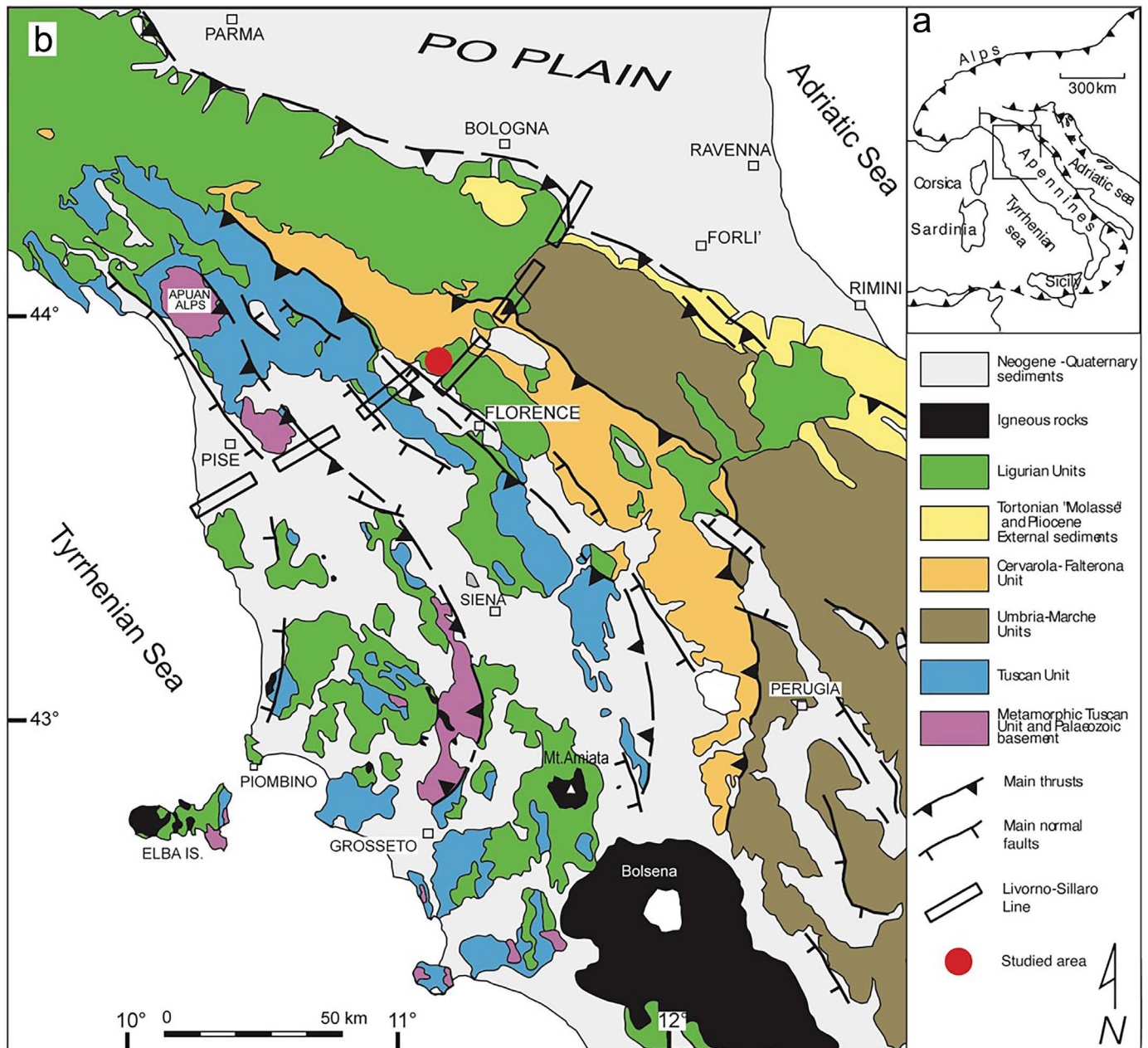
Fig. 2 - a) Inset of the Alps-Apennines region and its tectonic elements. b) Simplified geological sketch-map of the Northern Apennines. The circle marks the area of the Monteferrato ophiolite near Prato (modified from Sani et al., 2016).

of abundant sedimentary ophiolitic breccias within the Ligurian Units (Argnani et al., 2004; Principi et al., 2004; Nirta et al., 2007).

From the Late Cretaceous to the Eocene, the opening of the Northern Atlantic Ocean and the northward drifting of Africa led to the closure of the Liguria-Piemonte Ocean, with the associated formation of Alpine (north-verging) and Apennine (south-verging) orogenic chains (Principi and Treves, 1984; Molli, 2008; Vignaroli et al., 2008). In the late Eocene, after the continental collision, the opening of the Balearic basin, associated with the counter-clockwise rotation of the Corsica-Sardinia block and the opening of the Tyrrhenian basin, led to the present tectonic form of the Northern Apennines (Marroni et al., 2017).

During compressive tectonic phases of the Apennines, slices of the Ligurian ophiolites have been incorporated into the outermost units: The Monteferrato Ophiolite is located in

the lowermost portion of the Monte Morello Ligurian Unit (Principi and de Luca-Cardillo, 1975). This ophiolitic body, however, does not preserve clear evidence to define the nature of its contact with overlying formations, whether sedimentary or tectonic.

Historically, the ophiolites cropping out in the area of Monteferrato (Fig. 3) were described by Targioni Tozzetti (1768), Repetti (1835), Savi (1839), and studied in more detail by De Bardi (1810), Capacci (1881), Cossa (1881), Panichi (1904; 1909), Steinmann (1913), Franceschini (1928), Capedri (1966) and Franzini et al. (1978). De Stefani (1881) and Lotti (1908) made the first regional maps. Steinmann (1913) described these rocks as a type example of his proposed 'Trinity' of serpentinites, gabbros, and cherty sediments, the foundation for his hypothesis that ophiolite assemblages had formed in a deep-sea environment. Merla et al. (1967) mapped the Sheet 106 (Firenze) of the Geological Map of

Table 1 - Main monuments with Verde Prato ornamental stone in the cladding and year of construction.

Monument	Year
San Miniato al Monte Basilica (Florence)	1013
Badia Fiesolana (Fiesole)	1028
Church of Sant'Ippolito a Piazzanese (Prato)	1050
Badia di Vaiano (Prato)	1075
San Fabiano (Prato)	1082
Santissimi Apostoli (Florence)	1090
Santo Stefano al Ponte (Florence)	1116
Collegiata (Empoli)	1119
San Zeno Cathedral (Pistoia)	1130
San Bartolomeo a Pantano (Pistoia)	1150
Saint John Baptistery (Florence)	1150
Cathedral (Prato)	1160
Federico II Castle (Prato)	1240
Santa Maria Novella Basilica (Florence)	1279
San Francesco (Prato)	1280
Santa Maria del Fiore Cathedral (Florence)	1296-1412
Saint John Baptistery (Pistoia)	1301
Giotto's Bell Tower (Florence)	1359
Santa Maria Novella Basilica (Firenze) - façade	1350-1920
Cathedral (Prato) - façade	1400
Basilica delle Carceri (Prato)	1400
Santa Croce Basilica (Florence) - façade	1863
Santa Maria del Fiore Cathedral (Florence) - façade	1871
Franciscan Monastery of Bethlehem (Prato)	1880

Italy at the scale 1:100,000 that includes the Monteferrato area. In their Explanatory Notes, they reported serpentinites, gabbros, diabases, ophiolitic breccias, and ophicalcites. Principi and De Luca-Cardillo (1975) further confirmed this geological setting. This typical ophiolitic sequence is overlain by an oceanic sedimentary sequence consisting of Monte Alpe Cherts, Calpionella Limestones and Palombini Shales, in turn covered by the flysch of the Calvana Supergroup formations (Abbate and Sagri, 1970; Boccaletti and Coli, 1983; Abbate et al., 1994), later referred to as the Monte Morello Unit.

In the new Regional Geological Map (CARG, 2012), surveyed at the scale 1:10,000, the Monteferrato Ophiolite consists of (Fig. 3):

– a main body of serpentinite that preserves relict portions, ranging in size from 1 m³ to 10s m³, of the peridotite protolith;

– gabbro intrusive into the original peridotite;

– basalt dykes (only two found in the whole area) that intrude both gabbros and ultramafics;

– massive basalts;

– pillow basalts interlayered with early beds of radiolarian cherts (Monte Alpe Cherts).

The great abundance of variously serpentinized peridotites (Fig. 3) intruded by moderate volumes of gabbros and local dykes, covered by basalts, together with the absence of a sheeted dyke complex do not meet the traditional "Penrose-type" definition for oceanic crust (Anonymous, 1972). While "Penrose crust" approximates the structure of oceanic crust developed in fast-spreading, non-rifted ridges (McClain, 2003), the Monteferrato Ophiolite internal structure, like many Northern Apennines ophiolites, better typifies the ocean crust that forms in slow-spreading peri-continental positions adjacent to rifted continental margins (Marroni et al., 1998; Rampone and Piccardo, 2000; Montanini et al., 2012).

PETROGRAPHY OF THE UNDEFORMED SERPENTINIZED PERIDOTITES OF "VERDE PRATO"

Orlandi (1976) did the first detailed analysis of the petrographical characteristics of the Monteferrato ophiolite. In that study, mainly focussed on a secondary garnet (andradite) discovered in the Volpaia quarry (cf., Fig. 3), the Author described the serpentinite as a homogeneous rock, dark green in colour, crosscut by occasional veins of talc, chrysotile, calcite and aragonite. In addition to a primary sulphide mineralization, mainly consisting of pyrrhotite, he also reported a more widespread network of secondary composite veins mainly consisting of diopside as aggregates of white needles, tremolite as both "hair-like" crystals and fibre aggregates ("byssolite" var.), andradite garnet and chlorite. Usually, the inner portion of this composite vein was found to consist of diopside or tremolite, whereas chlorite occurred at the serpentinite contact where garnet was observed to overgrow chlorite. The presence of calcic minerals indicated Ca-metasomatism, and their arrangement suggested they were rodingites. Rare marcasite, sphalerite, titanite, magnetite, pyrite were also sporadically found.

For the present study, we collected 12 samples from the historical and best-exposed Guarino quarry located in the NW part of the Monteferrato ophiolitic body, from which blocks of "Verde Prato" to be used for conservation purposes are still available. During sample collection, we focused on the large blocks of massive less deformed serpentinized peridotites (Fig. 4). In the quarry, used until 1995 to produce gravels for road embankments, the most massive blocks have been piled up in the yard (Fig. 4a) because of their poor commercial value.

In spite of their pervasive serpentinization, the massive blocks preserve the original mantle peridotite's microstructure. As evident in hand samples (Fig. 4b), the brownish domains are pseudomorphs after olivine whereas the greenish regions are pseudomorphs after pyroxenes.

The petrographic study was carried out on representative samples of the Guarino quarry from which polished thin sections (30 μm thick) were prepared. Thin sections were examined by means of a Zeiss WL polarized-light microscope and photomicrographs were taken with an Olympus BX41-P polarized-light microscope equipped with a digital camera.
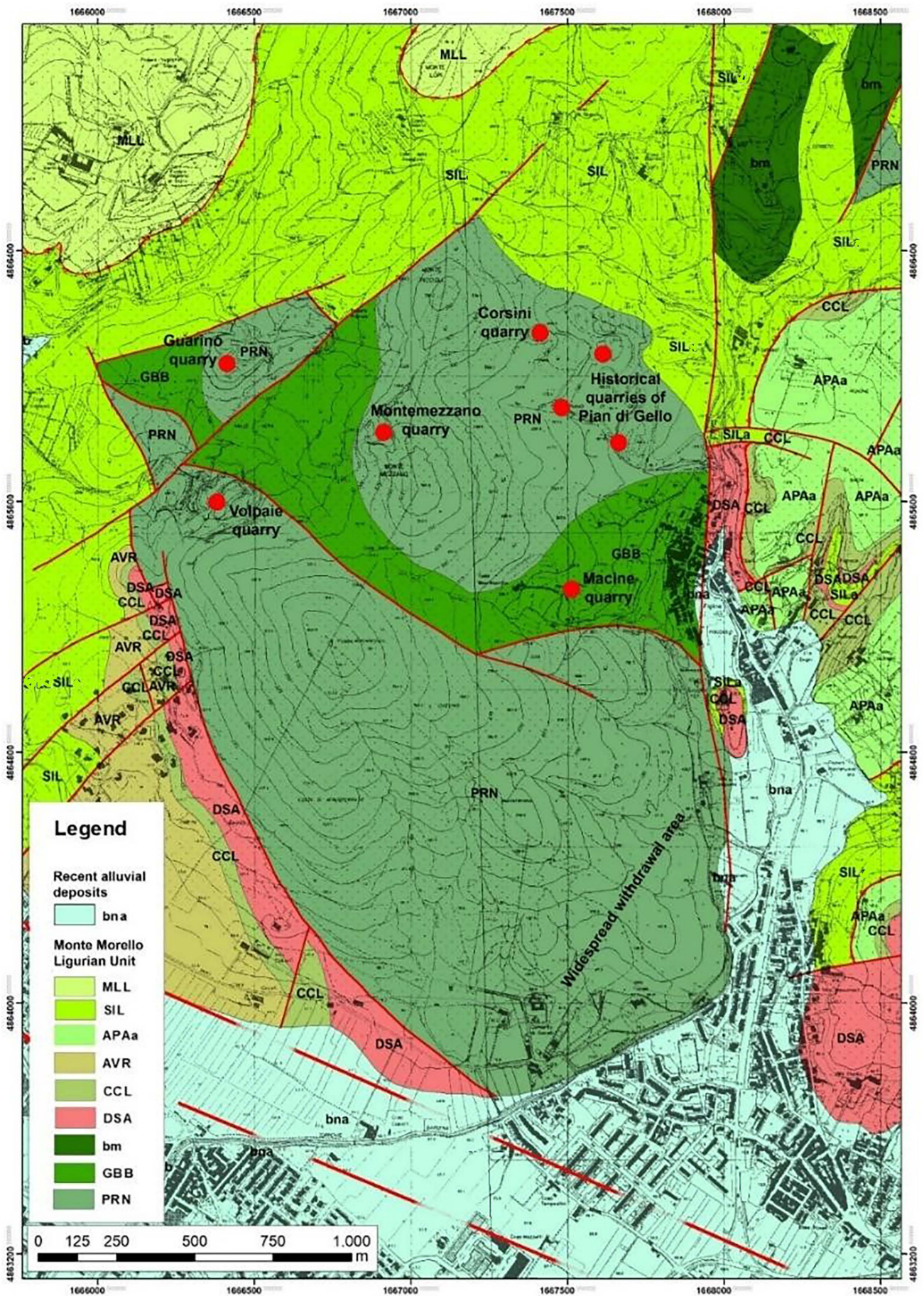
Fig. 3 - Geological map of the Monteferrato area north of Prato, Italy, showing the ophiolite body and its sedimentary cover (from CARG, 2012). MLL: Monte Morello Fm.; SIL: Sillano Fm.; APAa: Palombini Shales; AVR: Varicoloured Shales; CCL: Calpionella Limestones; DSA: Monte Alpe Cherts; bm: Basalts; GBB: Gabbros; PRN: Serpentinites with relict bodies of serpentinized peridotites. Dots: location of the main quarries. Red dashed lines: main faults.
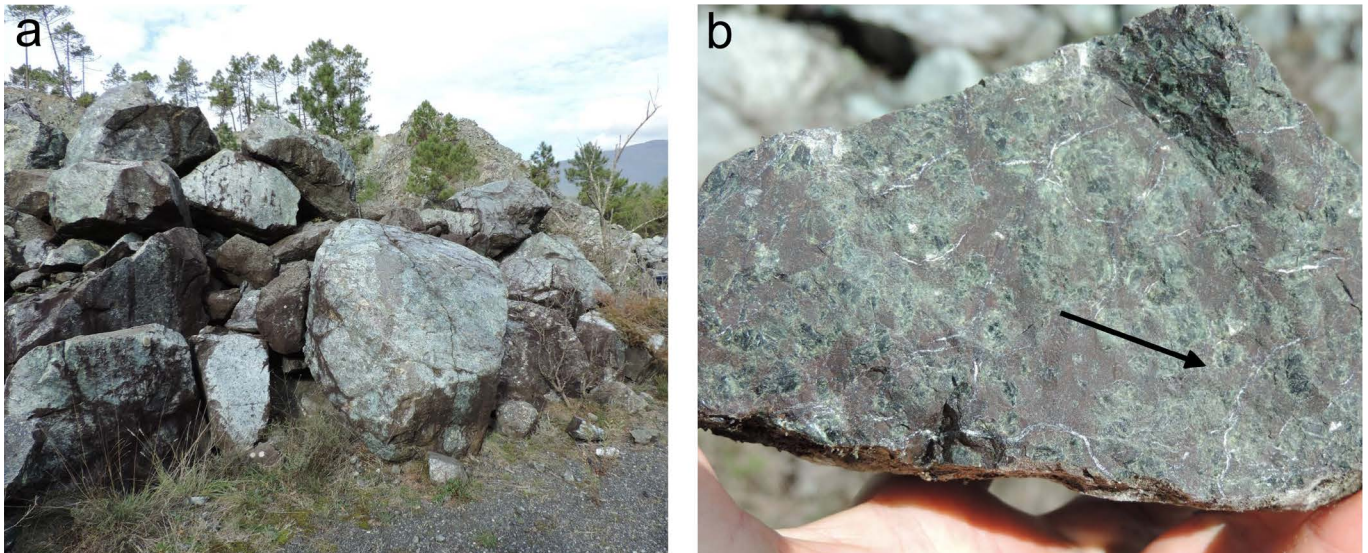
Fig. 4 - a) Accumulation of roundish blocks in the Guarino Quarry. These blocks are the most massive and least deformed portions of the serpentinized peridotites. b) Representative hand specimen of a wholly serpentinized peridotite: The red-brownish portions are pseudomorphs after olivine and greenish ones are pseudomorphs after pyroxenes. The discontinuous white veinlets are made of "cross" chrysotile (black arrow). The reader is referred to the PDF of the article for a colour version.

To evaluate the degree of rock deformation, three thin sections, cut perpendicular to each other, were made from the representative sample shown in Fig. 4b. Examination of the six photomicrographs of Fig. 6 confirms that the rock is isotropic and still preserves its original high-T peridotitic microstructure.

On the base of the different pseudomorph characteristics, the original sites of olivine, pyroxenes (orthopyroxene and possibly clinopyroxene), and spinel (now mainly opaque ore) were identified and their detailed description is reported below.

Pseudomorphs after olivine

The most widespread domains consist of a fine-grained greenish to brownish intimate aggregate of serpentine and opaque phases, usually magnetite (Figs. 5a to f, and 6a). The enlargement of these domains shows a "mesh" microstructure typical of olivine serpentinization (Fig. 6b), where the μ-Raman spectroscopy (see Section "Micro-Raman Spectroscopy") identified lizardite in the central brownish portion, surrounded by a colourless corona of chrysotile. At micro-Raman spectroscopy (μR) the fine-grained opaque phases were identified as magnetite (Fig. 8d) partly oxidized to hematite (Fig. 8e).

Pseudomorphs after orthopyroxene

A second domain, very poor in opaque ores, is the typical serpentine pseudomorph after orthopyroxene known as "bastite" that preserves the original regular "parting" of pyroxene and mimics the straight extinction of the original crystal (Fig. 6a). From μR analysis the whole pseudomorph is lizardite. A different orthopyroxene alteration, observed in a few samples, consists of a complete replacement of the mineral by a very fine-grained pinkish aggregate of lizardite (Fig. 6c), which includes small brownish grains, identified as andradite at μR (Fig. 8f), often defining subparallel alignments.

Pseudomorphs after possible clinopyroxene (Cpx)

A third colourless domain, lacking the regular "parting" of "bastite", has been tentatively interpreted as a pseudomorph after clinopyroxene (Cpx). This domain mostly consists of lizardite characterized by a single homogeneous extinction (Figs. 5a, c, e, and 6d). This domain, after the information obtained from the chemistry of the relict picotite (see Section "Relict dark reddish-brown spinel"), has been also considered a different type of pseudomorph after orthopyroxene.

Opaque phases (spinels)

At least two main types of spinel were observed: The first type, found only in two samples, is a dark reddish-brown spinel, whereas the second type is opaque. The first type looks like a relic of the original mantle mineralogy, as confirmed by the chemical analyses (see Section "Relict dark reddish-brown spinel"). The second type, which exhibits a variety of corroded habits, is systematically intergrown with domains of clear lizardite (Fig. 6e) considered pseudomorphous after former orthopyroxene (see e.g., Bédart et al., 2009, Fig. 5d). Most of these opaque ore-lizardite intergrowths have a roundish shape (Fig. 6e) in agreement with the isotropic rock microstructure.

The only exception, which caught our attention, was a single site where shards of corroded opaque remnants embedded in a clear lizardite domain show a rough preferred orientation that suggest an inherited relict anisotropy (Fig. 6f). Since also in this case the clear lizardite must be interpreted as deriving from a former orthopyroxene (see e.g., Bédart et al., 2009, Fig. 9d). This was tentatively considered as a pseudomorph after a former spinel + pyroxene intergrowth, i.e., the breakdown product of a primary mantle garnet decomposed during the exhumation from the garnet- to the spinel-peridotite facies (see e.g., Guarnieri et al., 2012). In SEM-EDS, this opaque has a chemical composition characterized by a systematic high silica content ($SiO_2 \approx 18$ wt.%), incompatible with the chemistry of the spinel group. Since both X-ray microdiffraction and μR analyses were unable to explain this anomaly, it was decided to study it in detail by means of high-resolution electron microscopy.

The dark reddish-brown spinel, the only mantle phase that has escaped extensive hydrothermal alteration, can provide useful information on nature and evolution of peridotite protolith (see e.g., Irvine, 1967; Dick and Bullen, 1984; Arai, 1992), we will devote a specific section to its description (see Section "Relict dark reddish-brown spinel").
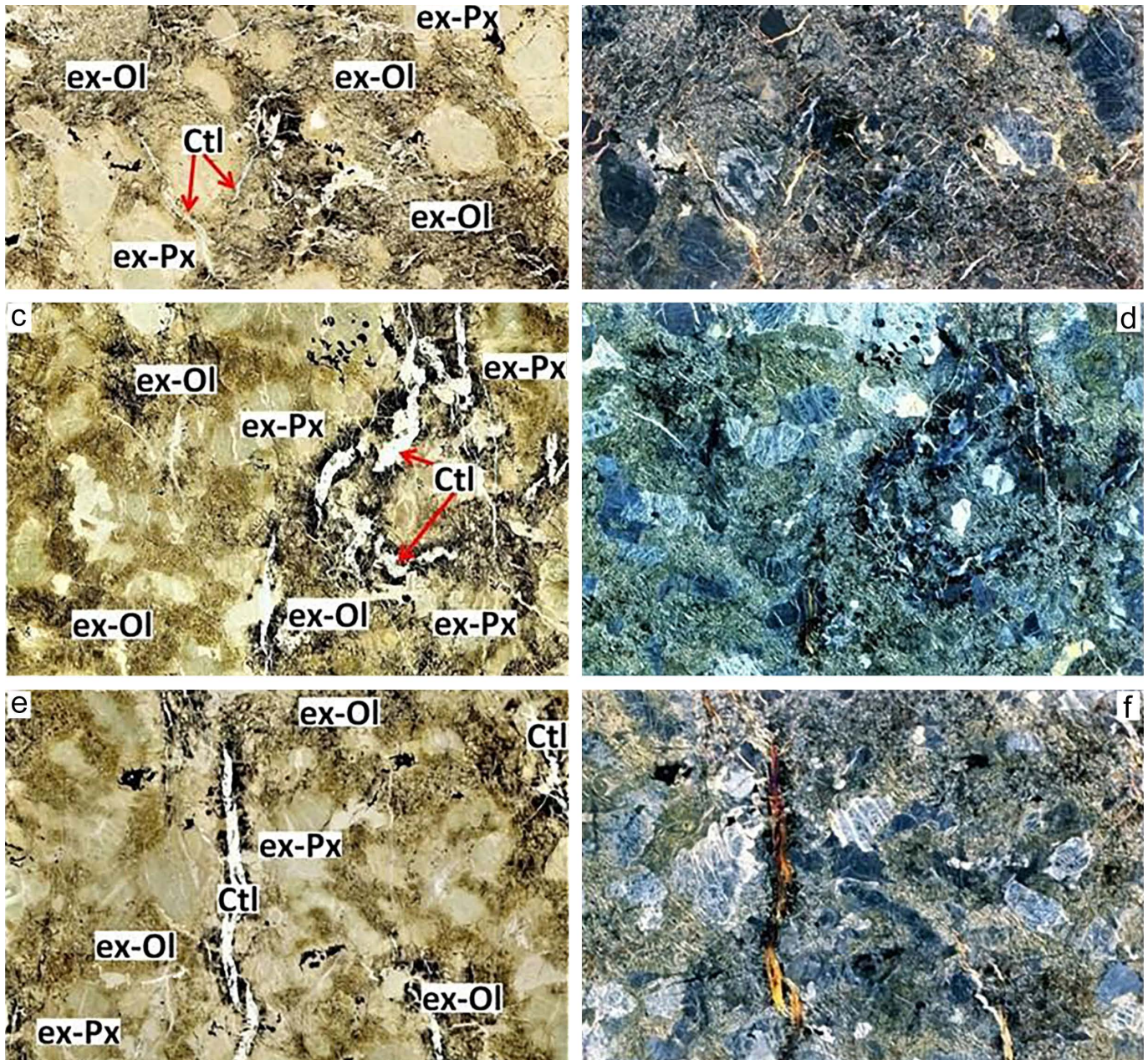
Fig. 5 - Photomicrographs of three thin sections, cut perpendicular to each other from the same sample. a), c), e) are observed under plane polarized light (PPL), and b), d), f) under crossed polarizers (XP), respectively. The isotropic microstructure of the peridotitic protolith and the pseudomorphic low-*T* alteration of the original mantle minerals is clearly visible. Primary olivine (ex-Ol: greenish domains in images a), c), e)) was replaced by a complex aggregate of lizardite ± magnetite, and pyroxenes (ex-Px: lighter domains at PPL) by light green to colourless lizardite that shows a single extinction under XP. Black spots at PPL are opaque ores. Note the thin veins of colourless chrysotile (Ctl) that are often bordered by black magnetite. Each image is 40 mm wide. The nature of the serpentine minerals was further checked by means of micro-Raman (µR) spectroscopy (see Section "Micro-Raman spectroscopy" and Fig. 8).

The veins

As already evident in hand samples, the serpentinized peridotite is cut by an irregular network of discontinuous colourless veins usually less than 1 mm thick of "cross" chrysotile (Figs. 5, 6c and f). Because of the systematic "cross" growth of chrysotile, in thin sections veins with different orientation can look very different in shape and optical characters. The veins that are cut perpendicular to the selvages but parallel to fibre elongation (Ctl // in Fig. 7a) appear thinner and more regular in thickness. Under crossed polarizers, they show relatively high interference colours (Fig. 7a). In contrast, the veins that are cut roughly parallel to the selvages and consequently perpendicular to the chrysotile fibres, appear lens-like in shape with very low interference colours (Ctl ⊥ in Fig. 7a), typical of a positive biaxial crystal (2Vγ = small) cut perpendicular to the acute bisector of the optical indicatrix. In addition to the ubiquitous chrysotile veins, thicker lizardite veins locally occur. These can be easily distinguished in thin section by their brownish-pinkish colour and extremely low interference colour (Liz in Fig. 7b). The crosscutting relationships between the two vein generations point to the earlier emplacement of chrysotile with respect to lizardite.

Lastly, layered mm-thick antigorite veins, confirmed by µR analyses, rarely occur (Fig. 8c). The examined thin sections do not constrain the precise crosscutting relationships of antigorite with lizardite and chrysotile veins.
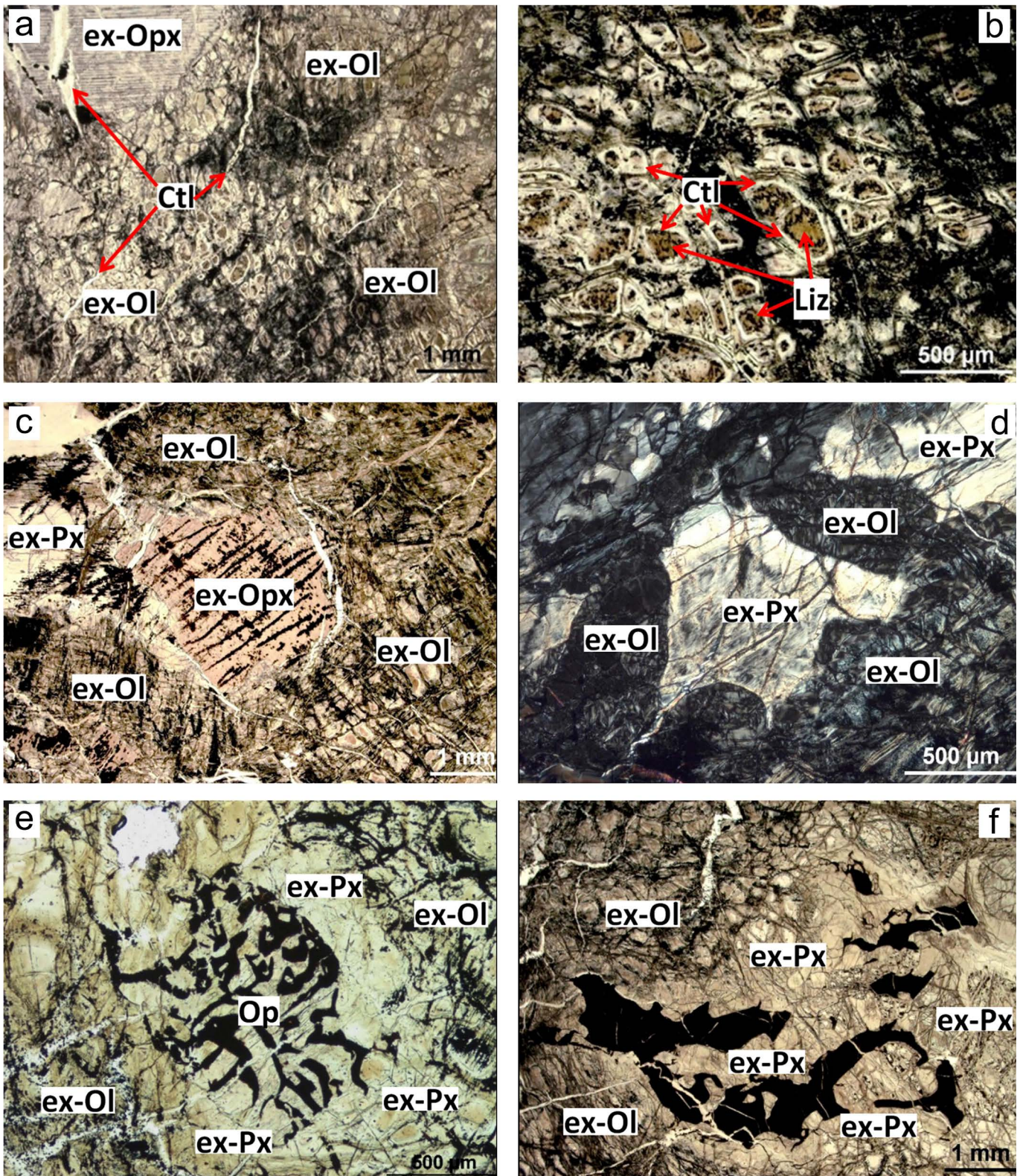
Fig. 6 - a) Photomicrographs (PPL) of a portion of the "mesh" serpentine after olivine (ex-Ol) and a "bastite" pseudomorph after former orthopyroxene with a regular "parting" (ex-Opx). White veinlets of chrysotile (Ctl) are also evident. b) Enlargement of the "mesh" microstructure (PPL Photomicrographs) after olivine that consists of optically isotropic brownish lizardite ± magnetite (Liz) domains surrounded by a thin colourless corona of chrysotile (Ctl). c) Photomicrograph (PPL) of another pseudomorph after orthopyroxene (ex-Opx) consisting of pinkish lizardite and semi-opaque alignments of very small andraditic garnet. d) Photomicrograph (XP) of a lizardite pseudomorph after former pyroxene (ex-Px), most likely orthopyroxene, surrounded by pseudomorphs after former olivine (ex-Ol). See text for further explanations. e) Photomicrograph (PPL) of a typical intergrowth of black spinel and clear lizardite after former pyroxene (ex-Px). Note the roundish shape of the intergrowth and corroded habit of black spinel (Op). f) Photomicrograph (PPL) of strongly corroded opaque shards with a rough preferred orientation, included in a clear lizardite pseudomorphous after former pyroxene (ex-Px). The black shards show a systematic high silica content (ca. 18 wt.%) incompatible with spinel chemistry. See text for further discussion. The reader is referred to the PDF of the article for a colour version.
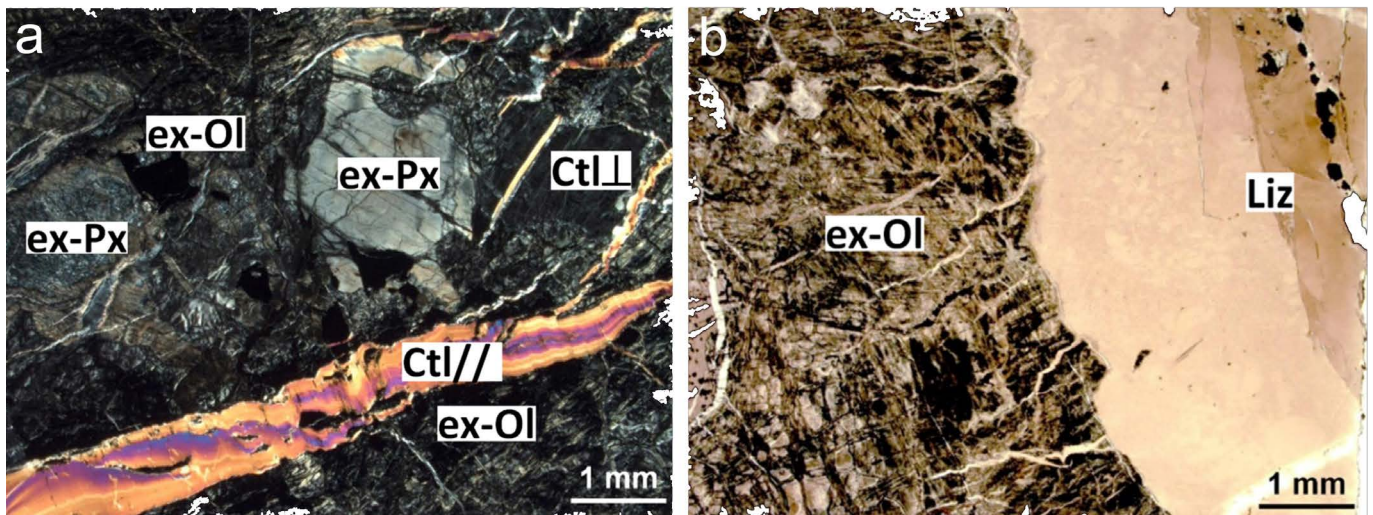
Fig. 7 - a) Photomicrograph showing veins of "cross" chrysotile cut ca. parallel (Ctl //) or perpendicular (Ctl ⊥) to mineral fibres. The different interference colours of Ctl // indicate an internal vein deformation. XP. b) Photomicrograph of a composite lizardite vein (Liz), characterized by different brownish colour depth, that is cutting a darker serpentinite mainly consisting of lizardite + Mt aggregates after former olivine (ex-Ol). PPL

MICRO-RAMAN SPECTROSCOPY

Petrographic observations were implemented by µR that, with its high-resolution power (ca. 1 µm), is the most suitable analytical technique for quick identification of the serpentine group minerals (Rinaudo et al., 2003; Groppo et al., 2006; Compagnoni et al., 2021) and of other mineral phases too fine-grained to be optically identified. Furthermore, this technique has the advantage that it can work on thin sections prepared for optical microscopy, allowing to identify the relationships between minerals and microstructures.

For each thin section, representative sites of minerals from different microstructures were analyzed by means of µR, whose spectra were acquired at the Dept. of Earth Sciences of the University of Turin, using a Horiba - Jobin Yvon HR800 LabRAM instrument equipped with a Nd-YAG laser (532 nm) 8mW power, an Olympus BX 40 optical microscope and a CCD detector cooled to -70°C by the Peltier effect. The analytical conditions were: 200 µm confocal hole, 100X objective lens (1 µm lateral spatial resolution), 1 cm^{-1} spectral resolution using 600 l/mm grid, 10 s and 10 reps. acquisition time on each spectrum. Correct calibration of the instrument was verified by checking the position of the Si band at 520.7 cm^{-1}. Spectra were processed using the Labspec 5 acquisition software. Raman spectra of hydrated minerals were acquired in the 70 - 4000 cm^{-1} range. Relevant representative patterns are shown in Fig. 8.

THE RELICT SPINEL

Petrographic and chemical data of dark reddish-brown spinel are from thin section FIB9, which contains two crystals, labelled FIB9_site1 and FIB9_site2, respectively.

Petrographic data

In thin section the two spinel crystals – ca. 0.70 mm and 1 mm long, respectively (Fig. 9a and b) exhibit a homogeneous dark reddish-brown colour (10R ¾ according to the Rock-colour Chart, 1995), with an opaque alteration rim of magnetite all along the crystal outlines and fractures (Fig. 9a and b). The most evident spinel fractures are filled by inner

lizardite (Fig. 9a and b) bounded by two discontinuous layers of magnetite (Fig. 9c).

Since during the polyphase serpentinization process the primary silicate minerals were completely replaced by lizardite and minor magnetite (tiny and white in Fig. 9c), the only relict dark reddish-brown spinel was analyzed to obtain information on the peridotite protolith.

Mineral chemistry

SEM-EDS data were acquired using a scanning electron microscope (JEOL JSM-IT300LV) equipped with an EDS Oxford Instruments X-act silicon drift detector, using AZtec 6.0 suite including QuantMap and AutoPhaseMap package. Operating conditions were: E = 15 KeV, WD = 10 mm, magnification = 50X (2.55 * 1.9 mm scanned area), 1024 x 768 pixels (resol = 2.5 μm), probe current = 5nA, process time = 1 μs (10^5 counts per second (CPS) with a dead time of 30%), SmartMap dwell time = 10 mSec.

For each crystal, a scan line along the major axis was analyzed, including 295 and 293 spot analyses, for FIB9_site1 and FIB9_site2, respectively. The average compositions of the two scan lines are reported in Table 2 left and the relevant atomic formulae in Table 2 right.

Atoms per formula unit (a.p.f.u.) were calculated based on four oxygens by means of the specific functions of Lanari et al. (2014), and the Fe^{2+} / Fe^{3+} ratio was obtained stoichiometrically.

Chemical compositions and structural formulae of the two spinels are reported in Table 2 left and right, respectively, and the structural formulae in Table 3.

In the trivalent Cr-Fe^{3+}-Al diagram of Guice et al. (2022), the FIB9 spinels plot in the field of picotite (Fig. 10) within the Cr-Al trend of ophiolites and oceanic peridotites as defined by Barnes and Roeder (2001). In the binary Cr# vs. Mg# diagram (Fig. 11) the FIB9 spinels plot in the field of Abyssal Peridotites of Bédard et al. (2009).

Because it is well known that the spinel chrome number Cr# = Cr/(Cr + Al), which is in the range 0.14-0.21 for lherzolites and 0.25-0.36 for harzburgites (Dick and Bullen, 1984; Hellebrand et al., 2001; Raye et al., 2011), reflects the degree of partial melting experienced by the peridotite, the FIB9 picotites with Cr# = 0.33-0.32 indicate a harzburgite protolith.
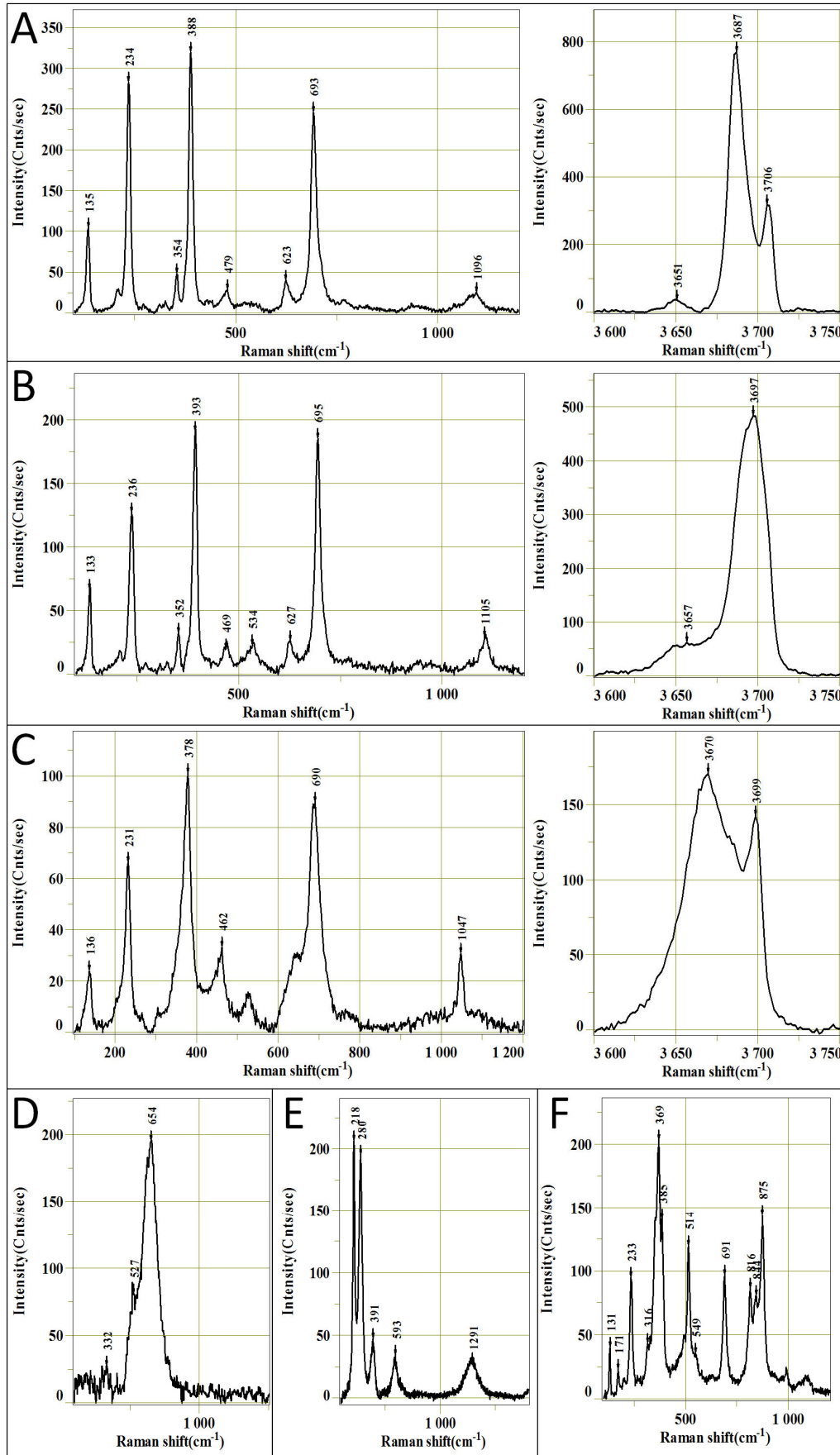
Fig. 8 - µ-Raman spectra of representative minerals from the "Verde Prato". For each mineral, the most intense and informative peaks are bracketed. a): Lizardite (3687, 3706 cm⁻¹); b) Chrysotile (1105, 3697 cm⁻¹); c): Antigorite (1047, 3670, 3699 cm⁻¹); d): Magnetite (654 cm⁻¹); e): Hematite (218, 280, 391 cm⁻¹); f): Andradite garnet (233, 369, 514, 691, 875 cm⁻¹). Sample identification - a) FIB3A Site2_1; b): FIB3A site 2_2; C: FIB6 Site 5_1; d): FIB8 Site 5_1; e): FIB 1 A Site 2_3; f): FIB 5 Site 1_2. The reader is referred to the PDF of the article for a colour version.
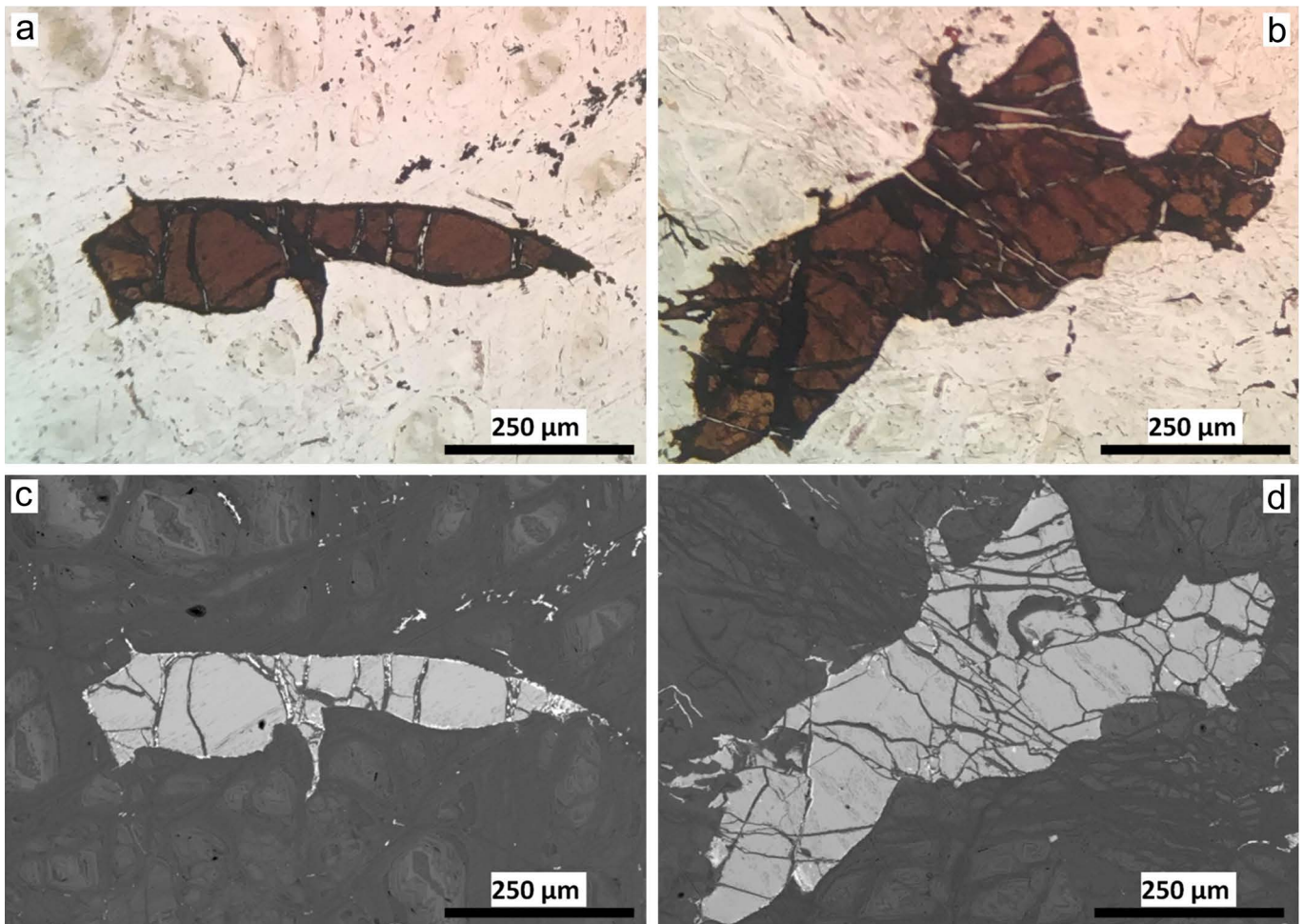
Fig. 9 - Photomicrographs under PPL (a and b) and Backscattered Electron (BSE) Images (c and d) of the two relict spinels from thin section FIB9, labelled FIB9_site1 (*left*) and FIB9_site2 (*right*), respectively. In A and B is evident the incipient opacization of the spinels along outlines and fractures, connected to the serpentinization process. The two relics are embedded in a lizardite groundmass developed at the expense of the former mantle silicates during a polyphase serpentinization process. In C and D the tiny thin white domains are magnetite.

Table 2 - Left: Average chemical compositions (wt. % oxide) of the two scan lines of the dark reddish-brown spinels including 295 (FIB9_L1) and 293 (FIB9_L2) spot analyses, respectively. Right: Structural formulae (a.p.f.u.) of the two spinels resulting from the mean chemical analyses.

	FIB9_L1		FIB9_L2			FIB9_L1		FIB9_L2	
Oxide	Avg (N=295)	Std. dev.	Avg (N=293)	Std. dev.	*Cation*	Avg (295)	Std. dev.	Avg (293)	Std. dev.
MgO	18.81	0.52	19.29	0.76	Mg	0.784	0.018	0.799	0.025
SiO_2	0.2	0.16	0.48	0.13	Si	0.006	0.004	0.013	0.004
Al_2O_3	37.57	1.14	37.63	1.29	Al	1.237	0.032	1.232	0.033
Cr_2O_3	26.84	1.08	27.46	1.35	Cr	0.593	0.027	0.604	0.036
FeO	16.03	0.71	15.1	0.74	Fe^{3+}	0.147	0.016	0.138	0.012
MnO	bdl		bdl		Fe^{2+}	0.227	0.02	0.213	0.025
Tot.	99.45		99.92						

bdl: below detection limit. Only significant oxides (in bold) were used for chemical formula calculation.

Applying the empirical equation by Hellebrand et al. (2001), which describes the extent of fractional melting (F) of mantle peridotites as a function of spinel Cr# [$F = 10 \ln$ (spinel Cr#) + 24], the FIB9 picotites yield estimates of ca. 13%

melting (Fig. 11), in the range of literature data for abyssal peridotites formed at slow spreading mid-ocean-ridges (Michael and Bonatti, 1985).
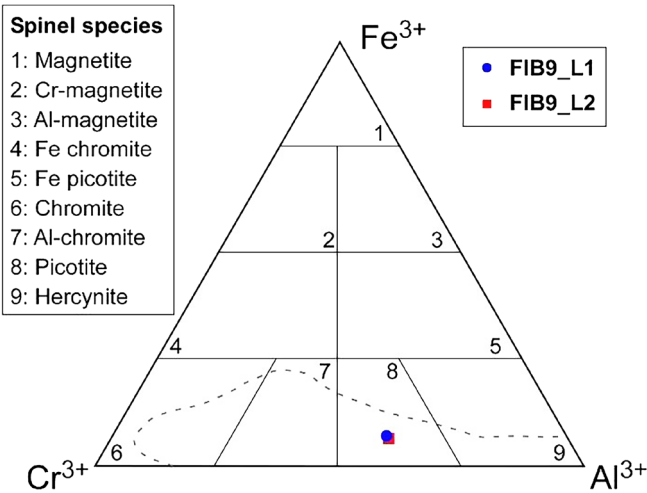
Fig. 10 - Classification and nomenclature of spinels in the ternary Fe^{3+}- Al - Cr^{3+} diagram (modified from Guice et al., 2022). The FIB9 relict spinels plot in the field of picotite. The dashed line delimits the the Cr-Al trend of ophiolites and oceanic peridotites as defined by Barnes and Roeder (2001).
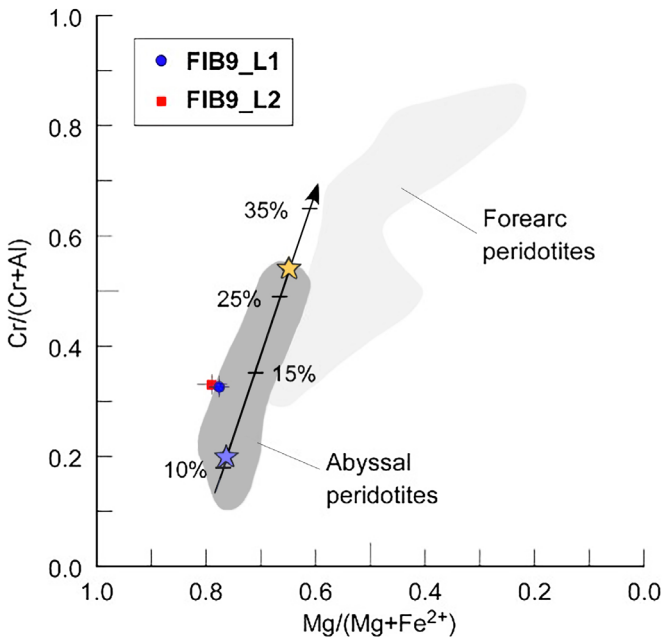

Fig. 11 - Cr# vs. Mg# binary plot for Cr-spinels. The FIB9 picotites plot in the field of Abyssal Peridotites. In the Mantle array, blue and yellow stars correspond to Mean MOR peridotite high-Al and low-Al spinels, respectively (Dick and Bullen, 1984). Compositional fields for abyssal and forearc peridotites are from Bédard et al. (2009). The partial melting degrees (in percent) are from the Hellebrand et al. (2001) calibration.

DISCUSSION

Our analysis, although limited, has shown that the Monteferrato serpentinized peridotites perfectly preserve the original isotropic microstructure. Since pseudomorphs after mantle pyroxenes show different types of low-T alteration, petrographic observations alone are insufficient to identify the peridotite protolith. However, the chemistry of relict picotite indicates with reasonable certainty that the "Verde Prato" serpentinite is derived from a former mantle harzbur-

gite that statically recrystallized in the spinel peridotite-facies field. We currently favour the hypothesis that the intergrowth of the opaque shards unusually high in silica with former orthopyroxene is derived by decomposition of garnet. If true, the strong overprint of a static spinel peridotite assemblage after a tectonitic garnet peridotite implies the following tectonic evolution:

1- decompression from ~ 2-2.5 GPa, i.e. ~ 70-80 km depths, to ~ 1.5 GPa, i.e. ~ 50 km depths – note that more precise equilibration conditions would require well-calibrated geothermobarometers that are beyond the scope of this study;

2- post-kinematic re-equilibration within the spinel-peridotite field during the decompression path and relict evidence of an early deformation recorded by the garnet peridotite. This indicates that the protolith of the Monteferrato serpentinite was deformed in its deepest recorded position and then exhumed with lower amounts of internal deformation.

This proposed evolution suggests that these peridotites represent vestiges of sub-continental mantle deformed in the early stages of lithosphere extension, that were then emplaced at shallower depths during continued extension and thinning of the overlying continental crust.

Interestingly, in other areas of the Northern Apennines the peridotites of the External Ligurian Units frequently occur in association with lower-crust granitic bodies (Bonatti, 1933; Merla, 1933; Bertolani, 1945; Giuseppetti, 1953; Fazzini and Tacoli, 1963; Bortolotti, 1964; Trevisan et al., 1971; Puccinelli et al., 2015). This suggests the close relationship of these peridotites with the continent and link their origin to a non-volcanic ocean-continent transition in the Ligurian Tethys margins (e.g., Molli, 1996; Marroni et al., 1998; 2017).

The evolution of the Monteferrato peridotites then continued with its pervasive low-T serpentinization characterized by olivine and pyroxenes replacement by lizardite and development of a network of early chrysotile and late lizardite veins. Rare antigorite veins were also found, although their crosscutting relationships with the other serpentine-bearing veins were not observed.

Both chrysotile and lizardite usually occur at $T < 300°C$ but their P-T-X conditions are still a matter of debate. Evans (2004) considers chrysotile as a metastable phase in veins that form under isotropic/low – and non-stable – stress conditions in cracks under high fluid pressure, while lizardite is stable under non-isotropic stress conditions and lower fluid pressure. Conversely, Viti and Mellini (1997) suggest that chrysotile vs. lizardite crystallization is controlled by differing chemical conditions. In the Monteferrato peridotites the systematic occurrence of chrysotile veins cut by lizardite veins would therefore suggest either a change in stress conditions during vein formation – from an isotropic shear stress environment dominated by cooling and water percolation to a tectonically active tectonic environment able to accommodate lizardite growth through expansion, i.e., an extensional tectonic environment – or a change in the cationic composition of circulating fluids. If chrysotile vs. lizardite crystallization in veins were controlled by shear stress conditions, then the Monteferrato peridotite, which was deformed at depths of ~ 70-80 km in the earliest stages of lithosphere extension and emplaced at the ocean-continent transition, would also record a second extensional deformation phase, after an interval of tectonic quiescence.

In addition to these veins, the presence of antigorite, stable at higher PT conditions could further complicate the picture. Antigorite occurrence could be related to early hydrothermal activity connected to gabbro intrusion (Frassi et al., 2022), or

to initial ocean floor serpentinization (Roumejon et al., 2015). The Monteferrato peridotites are indeed associated with gabbros (Fig. 2). In both cases, the antigorite veins should be the earliest veins within the Monteferrato peridotites. Another possibility could be related to prograde metamorphism, but this mechanism seems inconsistent with the regional thermal evolution. In fact, even assuming the possible subduction of the Monteferrato peridotites, its position in the external part of the Apennines would imply that it occurred under low-pressure conditions.

If the antigorite is related to oceanic hydrothermal activity and the chrysotile to lizardite crystallization is related to the activation of tectonic deformation in an extensional domain, then we can envisage different scenarios for the late evolution of the Monteferrato peridotites in the Ligurian Tethys. A possible evolution, following a hypothesis proposed in the 1980s, considers the Ligurian Tethys to be characterized by many transform faults that were active not only during the opening of the ocean, but also during its closure (Nirta et al., 2007). In this case, transform faults would be the dominant sites of mantle diapirism (Gianelli and Principi, 1977; Marcucci et al., 1982) with trans-tension possibly active at some stage of the ocean's evolution. If this is the case, diapirism or topographic highs related to transform faults/fracture zones systems could have triggered slope instabilities and the inclu-

sion of big masses of peridotites in the sedimentation basin of the Monte Morello Unit.

A second hypothesis would consider extension to be the product of bending of the ocean-continent transition area related to subduction of the Ligurian Ocean. Recently, Vannucchi et al. (2020) proposed that Apennine sub-continental serpentinized peridotites, related to the opening of a magma-poor rifted margin and exposed to the ocean floor, could be reactivated as diapirs during oceanic subduction. In this case bending of the subducting plate could reactivate the normal crustal faults of the passive margin and contribute to the diapirism of serpentinized peridotites. Once subducted the serpentinite diapirs could intrude the inner part of the accretionary prism, and eventually be embedded as shorn diapirs in the external part of the prism where mass wasting was also taking place (Vannucchi et al., 2020) (Fig. 12).

CONCLUSIONS

New mineralogical, petrographical and chemical analyses suggest that the Monteferrato ophiolites, containing also the serpentinitized peridotites of this study, are representative of oceanic crust originally located in a pericontinental position adjacent to the rifted margin in a slow-spreading
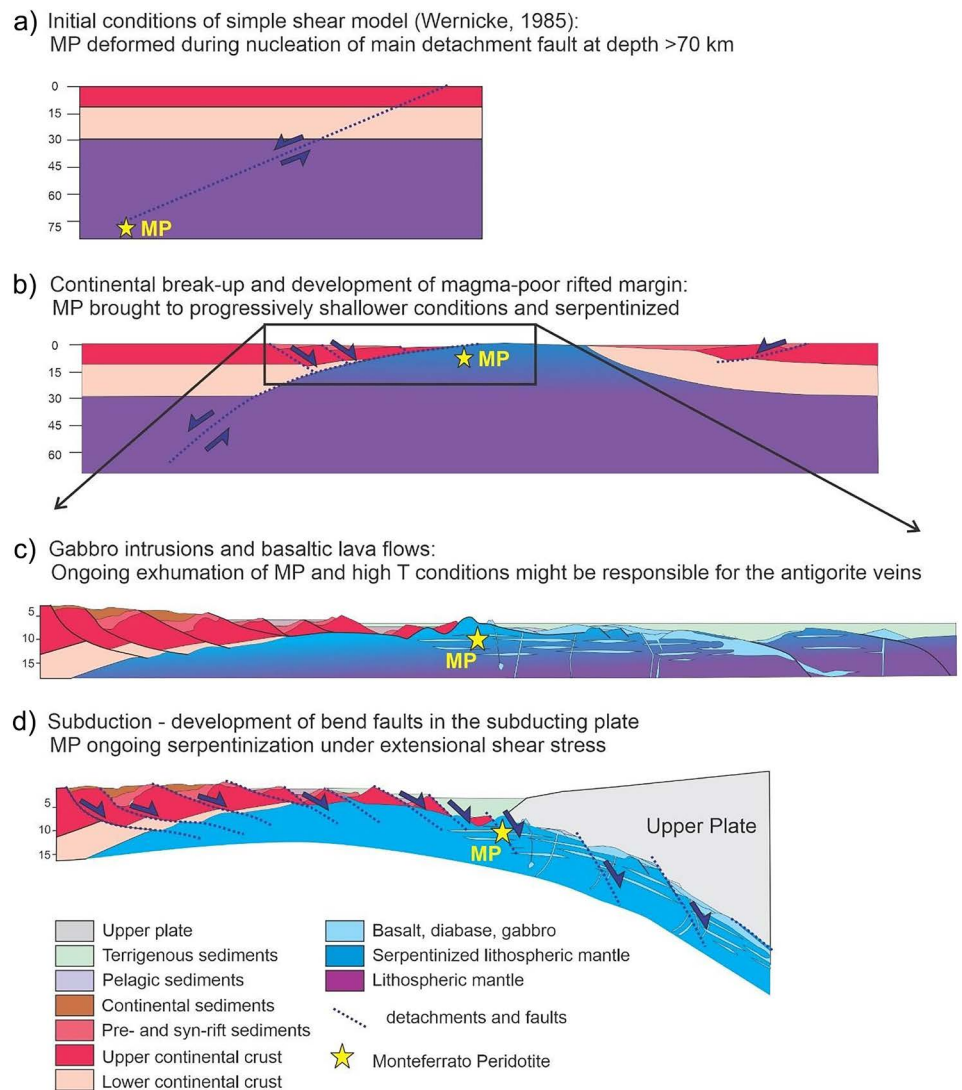

Fig. 12 - Cartoon illustrating the possible evolution path of the Monteferrato Peridotite (MP) since the Late Jurassic crustal extension for the opening of the Liguria-Piemonte Ocean to the Late Cretaceous-Eocene subduction bending and slice sampling within the base of the Monte Morello External Ligurian Unit. (Cartoon modified from Vannucchi et al., 2020).

ridge setting. The peridotites can be interpreted as a relic of sub-continental mantle deformed in the early stages of lithosphere extension that was then uplifted to a shallower depth by extreme thinning of the overlying continental crust. Subsequent/polyphase serpentinization processes may help to understand its relationship with the Monte Morello Unit. In fact the question regarding whether the ophiolite is the original substratum of the Monte Morello Unit, or if it is included in the sedimentary formations of Monte Morello Unit and how – through sedimentary or tectonic processes – are still a matter of debate due to lack of clear contacts. Here we propose that the Monteferrato serpentinized peridotites was uplifted to the ocean floor and the remobilized due to gravitational mechanism, whether related to slope instability or diapirism.

The serpentinized peridotites of Monteferrato also carries important meanings related to both its appearance in many historical monumental buildings of Tuscany, and for the history of geology, being one of the original outcrops that defined the "Steinmann Trinity", pivotal to understand ocean formation. Based on these reasons, we propose that the quarries of Figline di Prato exposing the Monteferrato peridotites should become a geosite of Tuscany. This proposition will need to be carefully assessed due to the frequent occurrence of chrysotile bearing veins, a fibrous mineral that is now recognized as being carcinogenic (IARC 1977; WHO, 1986). The content of chrysotile fibres in "Verde Prato" should therefore be properly quantified to check whether their number exceeds the upper limit deemed safe in current Italian regulations.

Finally, future studies of the Monteferrato peridotites should focus on decoding the meaning of its serpentinization, and deciphering its timing, nature and assessing the associated volume changes.

ACKNOWLEDGEMENTS

REFERENCES

Abbate E. and Bortolotti V., 1984. Le Unità Liguri dell'Appennino Settentrionale: sintesi dei dati e delle interpretazioni dal 1970. Mem. Soc. Geol. It., Cento Anni di Geologia Italiana 1881-1981, Vol. Giubilare, p. 215-240.

Abbate E. and Sagri M., 1970. The eugeosynclinal sequence. In: G. Sestini (Ed.), Development of the Northern Apennines geosyncline. Sedim. Geol., 4: 251-340.

Abbate E., Bortolotti V., Passerini P., Principi G. and Treves B., 1994. Oceanisation processes and sedimentary evolution of the Northern Apennine ophiolite suite: a discussion. Mem. Soc. Geol. It., 48: 117-136.

Abbate E., Bortolotti V. and Principi G., 1980. Apennine Ophiolites: a peculiar oceanic crust. Ofioliti, Spec. Iss., 1: 59-96.

Anonymous, 1972. Penrose Field Conference on ophiolites. Geotimes, 17: 24-25.

Arai S., 1992. Chemistry of chromian spinel in volcanic rocks as a potential guide to magma chemistry. Miner. Mag., 56: 173-784.

Argnani A., Fontana D., Stefani C. and Zuffa G.G., 2004. Late Cretaceous carbonate turbidites of the Northern Apennines: Shaking Adria at the onset of Alpine collision. J. Geol., 112 (2): 251-259.

Barnes S.T. and Roeder P.L., 2001. The range of spinel compositions in terrestrial mafic and ultramafic rocks. J. Petrol., 42 (12): 2279-2302.

Bastogi M. and Fratini F., 2004. Geologia, litologia, cave e deterioramento delle pietre fiorentine. Mem. Descr. Carta Geol. d'It., 66: 27-42.

Bédard É., Hébert R., Guilmette C., Lesage G., Wang C.S. and Dostal J., 2009. Petrology and geochemistry of the Saga and Sangsang ophiolitic massifs, Yarlung Zangbo suture zone, Southern Tibet: evidence for an arc-back-arc origin. Lithos, 113: 48-67.

Bertolani M., 1945. Contributo alla conoscenza della formazione ofiolitica appenninica. Graniti erratici dell'Appennino Modenese. Atti Soc. Nat. Mat. Modena, Processi Verb. Adunanze, 76: 23-39.

Boccaletti M. and Coli M., 1983. La tettonica della Toscana: assetto ed evoluzione. Mem. Soc. Geol. It., 25: 51-62.

Boccaletti M., Coli M., Principi G., Sagri M. and Tortorici L., 1984. Piedmont-Ligurian Ocean: an example of passive tension fissure within a mega-shear zone. Ofioliti, 9 (3): 353-362

Bonatti S., 1933. Studio petrografico dei graniti della formazione ofiolitica appenninica. Boll. R. Uff. Geol. d'It., 58: 7-10.

Bortolotti V., 1964. Geologia dell'alta Garfagnana tra Poggio, Dalli e Gramolazzo. Boll. Soc. Geol. It., 83: 25-154.

Capacci C., 1881. La formazione ofiolitica del Monteferrato presso Prato (Toscana). Boll. R. Comit. Geol. d'It., 12: 275-312.

Capedri S., 1966. Ricerche petrografiche sulle rocce ofiolitiche del Monteferrato (Prato), Atti Soc. Tosc. Sci. Nat., Serie A, 73 (1): 192-231.

CARG, 2012. Cartografia Geologica Regione Toscana, continuum geologico in scala 1:10,000. Regione Toscana. http://www.lamma.rete.toscana.it/carta-geologica-1-10000.

Compagnoni R., Cossio R. and Mellini M., 2021. Raman anisotropy in serpentine minerals, with a caveat on identification. J. Raman Spectr., 52: 1334-1345.

Cossa A., 1881. Sulla massa serpentinosa del Monte Ferrato (Prato). Boll. R. Com. Geol. d'It., 12: 240 pp.

De Bardi G., 1810. Osservazioni mineralogiche sopra alcuni luoghi adiacenti alla pianura di Prato. Opuscoli, Prato, p. 163-192.

De Stefani C., 1881. Quadro complessivo dei terreni che costituiscono l'Appennino Settentrionale. Mem. Soc. Tosc. Sci. Nat., 5: 206-254.

Dick H.J.B. and Bullen T., 1984. Chromian spinel as a petrogenetic indicator in abyssal and Alpine-type peridotites and spatially associated lavas. Contr. Miner. Petrol., 86: 54-76.

Elter P., 1975. L'ensemble ligure. Bull. Soc. Géol. Fr., 17: 984-997.

Evans B.W., 2004. The serpentinite multisystem revisited: Chrysotile is metastable. Int. Geol. Rev., 46 (6): 479-506.

Fazzini P. and Tacoli M.L., 1963. La serie oligo-miocenica del versante padano dell'Appennino Settentrionale e la sua posizione nella tettonica regionale. Atti Soc. Nat. Mat. Modena, Processi Verbali Adunanze, 94: 33-52.

Franceschini F., 1928. Brevi cenni intorno al Monteferrato nel distretto di Prato, Firenze. Stabilimento fiorentino d'arte grafica, 4 pp.

Franzini M., Leoni L., Mellini M. and Orlandi P., 1978. The babingtonite of Figline (Prato, Italy). Rend. Soc. Ital. Miner. Petrol., 34 (1): 45-50

Frassi C., Chighine G., Mauro D., Biagioni C., Zaccarini F. and Marroni M., 2022. Pervasive crystallization of antigorite in Northern Apennine ophiolites: the example of Montecarelli peridotites (Tuscany, Central Italy). Ofioliti, 47 (1): 37-49, doi: 10.4454/ofioliti.v47il.550

Fratini F. and Rescic S., 2013. The stone of the historical architecture of Tuscany, Italy. In: J. Cassar, M.G. Winter, B.R. Marker, N.R.G. Walton, D.C. Entwisle, E.N. Bromhead and J.W.N. Smith (Eds.), Stone in historic buildings: Characterization and performance. Geol. Soc. London Spec. Publ., 391. http://dx.doi.org/10.1144/SP391.5

Gianelli G. and Principi G., 1977. Northern Apennines ophiolites: an ancient transcurrent fault zone. Boll. Soc. Geol. It., 96: 53-58.

Giuseppetti G., 1953. Rocce e minerali della formazione ofiolitica di Volpedo (Oltrepò pavese). Rend. Soc. Miner. It., 9: 85-134.

Groppo C., Rinaudo C., Cairo S., Gastaldi D. and Compagnoni R., 2006. Micro-Raman spectroscopy for a quick and reliable identification of serpentine minerals from ultramafics. Eur. J. Miner., 18: 319-329.

Guarnieri L., Nakamura E., Piccardo G.B., Sakaguchi C., Shimizu N., Vannucci R. and Zanetti A., 2012. Petrology, trace elements and Sr, Nd, Hf isotope geochemistry of the North Lanzo Peridotite Massif (Western Alps, Italy). J. Petrol., 52 (11): 2259-2306.

Guice G.L., Reis Magalhães J., Piacentini Pinheiro M.A., Carolini Ramos Ferreira R., Tieppo Meira V., Melo-Silva P. and Ackerson M.R., 2022. Spinel-group minerals as a record of magmatic and metamorphic processes: evidence from the highly altered Morro do Onça ultramafc suite, São Francisco Craton (Brazil). Contr. Miner. Petrol., 177, 34. https://doi.org/10.1007/s00410-022-01901-0

Hellebrand E., Snow J.E., Dick H.J.B. and Hofmann A.W., 2001. Coupled major and trace elements as indicators of the extent of melting in mid-ocean-ridge peridotites. Nature, 410: 677-681.

IARC (International Agency for Research on Cancer), 1977. Monographs on the evaluation of the carcinogenic risk of chemicals to man: asbestos. 14th Edn.

Irvine T.N., 1967. Chromian spinel as a petrogenetic indicator. Part 2. Petrologic applications. Can. J. Earth Sci., 4: 71-103.

Lagabrielle Y. and Cannat M., 1990. Alpine Jurassic ophiolites resemble the modern central Atlantic basement. Geology, 18: 319-322.

Lanari P.O., De Andrade V., Dubacq B., Lewin E., Eugene G., Grosch E.G. and Schwartz S., 2014. XMapTools: A MATLAB©-based program for electron microprobe X-ray image processing and geothermobarometry. Comput. Geosci., 62: 227-240.

Lotti B., 1908. Cenni sulla geologia della Toscana. Boll. R. Com. Geol. d'It., 4: 1-28.

Malesani P., Pecchioni E., Cantisani E. and Fratini F., 2003. Geolithology and provenance of materials of some historical buildings and monuments in the center of Florence (Italy). Episodes, 26 (3): 250-255.

Marcucci M., Passerini P. and Sagri M., 1982. Northern Paleo-Apennine: subduction or scattered crumpling? Modern Geol., 8: 107-113.

Marroni M. and Pandolfi L., 2007. The architecture of the Jurassic Ligure-Piemontese oceanic basin: tentative and reconstruction along the Northern Apennine - Alpine Corsica transect. Int. J. Earth Sci., 96: 1059-1078.

Marroni M., Meneghini F. and Pandolfi L., 2017. A revised subduction inception model to explain the Late Cretaceous, double-vergent orogen in the pre-collisional western Tethys: Evidence from the Northern Apennines. Tectonics, 36: 2227-2249, doi 10.1002/2017TC004627.

Marroni M., Molli G., Montanini A. and Tribuzio R., 1998. The association of continental crust rocks with ophiolites in the Northern Apennines (Italy): implication for the continent-ocean transition in the Western Tethys. Tectonophysics, 292: 43-66

Marroni M., Molli G., Montanini A., Ottria G., Pandolfi L. and Tribuzio R., 2002. The External Ligurian Units (Northern Apennine, Italy): From rifting to convergence of a fossil ocean-continent transition zone. Ofioliti, 27 (2): 119-132.

McClain J., 2003. Ophiolites and the interpretation of marine geophysical data: How well does the ophiolite model works for the Pacific Ocean crust? Geol. Soc. Am. Spec. Pap., 373: 173-185, doi: 10.1130/0-8137-2373-6.173

Merla G., 1933. I graniti della formazione ofiolitica appenninica. Boll. R. Uff. Geol. d'It., 58 (6): 116 pp.

Merla G., Bortolotti V. and Passerini P., 1967. Note illustrative della carta geologica d'Italia alla scala 1:100.000. Foglio 106 (Firenze). Servizio Geologico d'Italia, Roma. Nuova Tecnica Grafica, Roma, 61 pp.

Michael P.J. and Bonatti E., 1985. Peridotite composition from the North Atlantic: regional and tectonic variations and implications for partial melting. Earth Planet. Sci. Lett., 73 (1): 91-104. https://doi.org/10.1016/0012-821X(85)90037-8

Molli G., 1996. Pre-orogenic tectonic framework of the Northern Apennine ophiolites. Ecl. Geol. Helv., 89 (1): 163-180.

Molli G., 2008. Northern Apennine–Corsica orogenic system: an updated overview. Geol. Soc. London Spec. Publ., 298 (1): 413-442.

Montanini A., Tribuzio R. and Thirlwall M., 2012. Garnet clinopyroxenite layers from the mantle sequences of the Northern Apennine ophiolites (Italy): Evidence for recycling of crustal material. Earth Planet. Sci. Lett., 351-352: 171-181.

Nirta G., Principi G. and Vannucchi P., 2007. The Ligurian Units of Western Tuscany (Northern Apennines): Insight on the influence of pre-existing weakness zones during ocean closure. Geodin. Acta, 20 (1-2): 71-97.

Orlandi P., 1976. Il granato del Monte Ferrato ed i minerali che l'accompagnano. Atti Soc. Tosc. Sci. Nat., Mem. (Pisa), 81: 167-173.

Panichi U., 1904. Le rocce verdi di Monte Ferrato in Toscana. Atti R. Acc. Sci. Torino, 39 (1903-1904): 769-777.

Panichi U., 1909. Ricerche petrografiche, chimiche e geologiche sul Monte Ferrato (Toscana). Atti Soc. Tosc. Sci. Nat., Mem. (Pisa), 25: 3-20.

Principi G. and De Luca-Cardillo M., 1975. Nuovi dati preliminari sulla coltre alloctona a nord di Prato (Firenze). Boll. Soc. Geol. It., 94: 1199-1206.

Principi G. and Treves B., 1984. Il sistema Corso-Appenninico come prisma di accrezione. Riflessi sul problema generale del limite Alpi-Appennini. Mem. Soc. Geol. It., 28: 549-576.

Principi G., Bortolotti V., Chiari M., Cortesogno L., Gaggero L., Marcucci M., Saccani E. and Treves B., 2004. The pre-orogenic volcano-sedimentary covers of the Western Tethys oceanic basin: a review. Ofioliti, 29 (2): 177-211.

Puccinelli A., D'Amato Avanzi G. and Perilli N., 2015. Carta Geologica d'Italia alla scala 1:50.000, foglio 250 (Castelnuovo di Garfagnana), Note Illustrative. ISPRA, Roma, 166 pp.

Rampone E. and Piccardo G.B., 2000. The ophiolite-oceanic lithosphere analogue: New Insights from the Northern Apennines (Italy). In: Y. Dilek, E.M. Moores and D. Elthon (Eds.), Crust: New insights from field studies and the Ocean Drilling Program. Geol. Soc. Am., Spec. Pap., 349: 21-34. http://dx.doi.org/10.1130/0-8137-2349-3.21

Raye U., Anthony E.Y., Stern R.J., Kimura J-I., Ren M., Chang Q. and Tani K., 2011. Composition of the mantle lithosphere beneath south-central Laurentia: Evidence from peridotite xenoliths, Knippa, Texas. Geosphere, 7 (3): 710-723. https://doi:10.1130/GES00618.1

Repetti E., 1835. Dizionario geografico fisico e storico della Toscana - Vol. II. Tofani Ed., Firenze, 955 pp.

Rinaudo C., Gastaldi D. and Belluso E., 2003. Characterization of chrysotile, antigorite and lizardite by FT-Raman spectroscopy. Can. Miner., 41 (4): 883-890.

Rodolico F., 1965. Le pietre delle città d'Italia. Le Monnier, Firenze, 501 pp.

Roumejon S., Cannat M., Agrinier P., Godard M. and Andreani M., 2015. Serpentinization and fluid pathways in tectonically exhumed peridotites from the Southwest Indian Ridge (62-65 degrees E). J. Petrol., 56 (4): 703-734.

Sani F., Bonini M., Montanari D., Moratti G., Corti G. and Del Ventisette C., 2016. The structural evolution of the Radicondoli-Volterra Basin (Southern Tuscany, Italy): Relationships with magmatism and geothermal implications. Geothermics, 59: 38-55.

Sartori R., 2002. Pietre e "marmi" di Firenze, notizie storiche, antiche cave, genesi e presenza nei monumenti, Alinea, Firenze, 88 pp.

Savi P., 1839. Memorie per servire allo studio della costituzione fisica della Toscana. F.lli Nistri, Pisa, 122 pp.

Schettino A., Turco E., 2011. Tectonic history of the western Tethys since the Late Triassic. Geol. Soc. Am. Bull., 123 (1-2): 89-105.

Steinmann G., 1913. Über Tiefenabsätze des Oberjura im Apennin. Geol. Runds., 4: 572–575.

Targioni Tozzetti G., 1768. Relazioni d'alcuni viaggi fatti in diverse parti della Toscana per osservare le produzioni naturali, e gli antichi monumenti di essa. Vol. II, Stamperia Granducale, Firenze, 540 pp.

Treves B., 1984. Orogenic belts as accretionary prisms: the example of Northern Apennines (Northern Italy). Ofioliti, 9: 577-618.

Trevisan L., Dallan L., Federici P.R., Giglia G., Nardi R. and Raggi G., 1971. Carta Geologica d'Italia in scala 1: 100.000, Foglio 96 (Massa), Note Illustrative. Serv. Geol. d'It., 57 pp.

Tribuzio R., Thirlwall M.F. and Vannucci R., 2004. Origin of the gabbro-peridotite association from the Northern Apennine ophiolites (Italy). J. Petrol., 45 (6): 1109-1124.

Vannucchi P., Morgan J.P., Polonia A. and Molli G., 2020. The life cycle of subcontinental peridotites: From rifted continental margins to mountains via subduction processes. Geology, 48 (12): 1154-1158. https://doi.org/10.1130/G47717.1

Vignaroli G., Faccenna C., Jolivet L., Piromallo C. and Rossetti F., 2008. Subduction polarity reversal at the junction between the Western Alps and the Northern Apennines, Italy. Tectonophysics, 450 (1-4): 34-50.

Viti C. and Mellini M., 1997. Contrasting chemical compositions in associated lizardite and chrysotile in veins from Elba, Italy. Eur. J. Miner., 9 (3): 585-596.

Wernicke B., 1985. Uniform-sense normal simple shear of the continental lithosphere. Can. J. Earth Sci., 22 (1): 108-125.

WHO, 1986. Asbestos and other natural mineral fibres. Geneva, Switzerland: World Health Organization Environmental Health Criteria 35.